Sequence 18−29 on Actin: Antibody and Spectroscopic Probing of Conformational Changes†

Susan B. Adams‡ and Emil Reisler*,§

Department of Chemistry and Biochemistry and Molecular Biology Institute and Department of Biology, University of California, Los Angeles, California 90024

Received July 1, 1994; Revised Manuscript Received September 13, 1994⊗

ABSTRACT: Experimental evidence for the involvement of the 18−29 site within actin subdomain-1 in the actomyosin weak binding interface includes the inhibition of actomyosin ATPase activity by specific peptide antibodies [Adams, S., & Reisler, E. (1993) *Biochemistry 32*, 5051−5056] and by the *Dictyostelium* actin mutant D24H/D25H [Johara, M., *et al.* (1993) *Proc. Natl. Acad. Sci. U.S.A. 90*, 2127−2131]. In this work, the effect of the 18−29 peptide antibodies on the polymerization and conformation of actin has been characterized. Binding of antibody to the 18−29 site strongly inhibited the $MgCl_2$-induced polymerization of G-actin, had a much weaker impact on the $CaCl_2$ polymerization of actin, and showed very little effect on the NaCl polymerization of G-actin. These observations were linked to the binding of the 18−29 antibody to the different forms of actin. In sedimentation assays, the (18−29) IgG bound more strongly to Mg-F- and Mg-G-actins than to Ca-F- and Ca-G-actins, respectively. The binding of IgG to F-actin decreased sharply with an increase in ionic strength. Antibody binding to the 18−29 site induced conformational changes within the nucleotide cleft, both slowing the rate of nucleotide exchange and increasing the fluorescence intensity of actin-bound ϵATP. The increased fluorescence of a dansyl probe attached to Gln-41 and a pyrene probe attached to Cys-374 demonstrated that antibody binding also caused local perturbations in the DNase I loop of subdomain-2 and at the C-terminus of actin. These results are discussed in terms of actin plasticity and its implications for actomyosin interactions.

The central location of the nucleotide cleft in actin, surrounded by the four actin subdomains (Kabsch *et al.*, 1990), provides a structural framework for the sensitivity of actin monomer to the nucleotide and the divalent cation bound within the cleft. Substitutions of either nucleotide or divalent cation result in conformational changes within the actin structure that are transmitted some distance away from the cleft. These conformational changes may have important ramifications in actin-based functions.

Local conformational changes triggered by divalent metal substitution in the cleft have been detected in G-actin both at the C-terminus (Valentin-Ranc & Carlier, 1989) and in the DNase I loop of subdomain-2 (Strzelecka-Golaszewska *et al.*, 1993) by using proteolytic enzymes or monitoring covalently attached fluorescent probes. Notably, changes within the nucleotide cleft can also be transmitted through the filament structure, as seen in the different degree of twisting exhibited by Ca- and Mg-actin filaments (Orlova & Egelman, 1993). In addition, P_i release from the cleft, following ATP hydrolysis, has been shown to increase the filament flexibility and destabilize the long pitch monomer−monomer contacts between subdomain-2 residues in the DNase I loop and residues in subdomain-3 of the adjacent monomer (Orlova & Egelman, 1992). The opposite effect, namely, a cooperative stabilization of subdomain-2 and the actin filament, has been observed upon the binding of BeF_x, a P_i analog, in the nucleotide cleft (Combeau & Carlier, 1988; Orlova & Egelmen, 1993; Muhlrad *et al.*, 1994). Given this level of plasticity in the actin structure, it would not be surprising if the binding of proteins could also induce conformational changes in actin.

The binding of tropomyosin and myosin to actin filaments is known to alter their flexibility (Ishiwata & Fujime, 1971; Yanagida & Oosawa, 1978). The myosin-induced increase in actin flexibility has been proposed to occur through conformational changes in subdomain-2 (Orlova & Egelman, 1993). In addition to the impact of myosin on the filament structure, local conformational changes are induced by myosin in G-actin (Kasprzak, 1993). The polymerization of G-actin by S-1[1] may be due, in part, to such changes (Miller *et al.*, 1988).

The dynamic aspects of actin structure are important in the context of the recent effort to map the actomyosin interface and to derive a detailed structural description of the myosin crossbridge cycle. These studies, utilizing mostly actin mutants (Sutoh *et al.*, 1991; Johannes & Gallwitz, 1991; Aspenström & Karlsson, 1991; Cook *et al.*, 1993; Johara *et al.*, 1993) and antibodies against specific sites on actin

† This work was supported by USPHS Grant AR22031 and NSF Grant MCB9206789.

‡ Department of Biology.

§ Department of Chemistry and Biochemistry and Molecular Biology Institute.

⊗ Abstract published in *Advance ACS Abstracts,* November 1, 1994.

[1] Abbreviations: S-1, myosin subfragment-1; 18−29 peptide antibodies, affinity-purified IgG and F_{ab} fragments of polyclonal antibodies directed against sequence 18−29 (KAGFAGDDAPRAY) from the N-terminus of rabbit α-skeletal actin; ELISA, enzyme-linked immunosorbent assay(s); ATP, adenosine 5′-triphosphate; pyrenyl actin, actin labeled at Cys-374 with *N*-(1-pyrenyl)iodoacetamide; 5-IAF actin, actin labeled at Cys-374 with 5-(iodoacetamido)fluorescein; DED actin, actin labeled at Gln-41with dansylethylenediamine; EDTA, ethylenediaminetetraacetic acid; Mg-G (or F)-actin, actin with Mg^{2+} bound in the high-affinity cation site; Ca-G (or F)-actin, actin with Ca^{2+} bound in the high-affinity cation site.

0006-2960/94/0433-14426$04.50/0

(Mejean *et al.*, 1987; DasGupta & Reisler, 1989, 1992; Adams & Reisler, 1993), have focused on the electrostatic interaction sites for myosin on actin, namely, the sequences 1−7, 18−29, and 90−101. Each of these sites was implicated in the weak binding of myosin to actin in the presence of ATP and in the motile function of actin (Reisler, 1993; Johara *et al.*, 1993; Adams & Reisler, 1993; Miller & Reisler, 1994). However, the degree to which allosteric effects of mutations and antibodies contribute to the inhibition of actin function in these cases is yet to be assessed. Of particular interest in such considerations is the 18−29 site on actin. Peptide antibodies to this site inhibited the acto-S-1 ATPase activity more effectively than acto-S-1 binding in the presence of MgATP (Adams & Reisler, 1993). This suggests that some of the functional inhibition of actin by the antibodies might arise from the coupling between the 18−29 loop and other sites on actin and their consequent indirect perturbation by IgG.

In the present study, we have extended the characterization of the invariant 18−29 site to assess its connectivity with other sites on actin and its role in actin functions such as polymerization and nucleotide binding. By measuring the binding of 18−29 antibodies to actin, we show that the conformation of this region changes upon the replacement of calcium by magnesium in the high-affinity metal site. We also show that antibody binding to actin slows the rate of nucleotide exchange from G-actin. The 18−29 site also communicates with other, more distant sites, such as the C-terminus and the DNase I loop in subdomain-2 on actin.

MATERIALS AND METHODS

Reagents. Distilled and Millipore-filtered water and analytical grade reagents were used in all experiments. ELISA plates (Dynatech Immulon I) were purchased from Fisher Scientific Co. Papain, ATP, ϵATP, peroxidase-conjugated goat anti-rabbit IgG, cyanogen bromide-activated Sepharose, Sephadex G50-80, Freund's adjuvant, iodoacetic acid, and TLCK-treated α-chymotrypsin were purchased from Sigma Chemical Co. (St. Louis, MO). *N*-(1-Pyrenyl)-iodoacetamide, 5-(iodoacetamido)fluorescein, and dansylethylenediamine (DED) were obtained from Molecular Probes (Junction City, OR). ECL reagent for Western blotting detection was purchased from Amersham. Keyhole limpet hemocyanin and Aquacide II were purchased from Calbiochem (La Jolla, CA). Bradford protein assay solution and protein A−agarose were from Bio-Rad (Richmond, CA). The synthetic peptide used for the immunization of rabbits was purchased from the custom peptide synthesis facility at the University of California at San Diego. Bacterial transglutaminase was a gift from Ajinomoto Co. Inc. (Kawasaki, Japan).

Preparation of Proteins. Rabbit skeletal muscle actin was prepared in G-actin buffer (0.2 mM $CaCl_2$, 0.5 mM β-mercaptoethanol, 0.2 mM ATP, and 5 mM Tris (pH 7.6)) by the procedure of Spudich and Watt (1971). Subfragment-1 (S-1) was prepared by chymotryptic digestion of myosin (Weeds & Pope, 1977). Myosin was prepared as described by Godfrey and Harrington (1970). S-1 was dialyzed just prior to use against a low-salt buffer (10 mM KCl and 10 mM imidazole (pH 7.0)) that favored S-1 binding to actin. Wild-type yeast actin and the D24A/D25A yeast actin mutant, in which the Asp-24 and Asp-25 residues were replaced by alanines, were gifts from C. Miller. The mutant actin strain was generously provided by Drs. D. Drubin, D. Botstein, and K. Wertman.

Preparation of Peptide Antibodies. Polyclonal antibodies against the synthetic peptide, Lys-Ala-Gly-Phe-Ala-Gly-Asp-Asp-Ala-Pro-Arg-Ala-Tyr, corresponding to skeletal muscle α-actin residues 18−29 (Vandekerckhove & Weber, 1984) were prepared as previously described (Adams & Reisler, 1993). The actin affinity-purified IgG and F_{ab} were obtained as reported before (Adams & Reisler, 1993). Antibody titers were checked by ELISA. IgG and F_{ab} were dialyzed into 5 mM Tris (pH 7.6) and were spun in a Beckman airfuge just prior to use to remove any aggregates.

Preparation of Mg-G-Actin. Mg(ATP)-G-actin was prepared from Ca(ATP)-G-actin (<50 μM) by incubation with 50 μM $MgCl_2$ and 100 μM EGTA for 10 min (Kinosian *et al.*, 1991). The Mg-actin was then centrifuged through a syringe column of Sephadex G-50-80 equilibrated with Mg-G-actin buffer (50 μM $MgCl_2$, 100 μM EGTA, and 5 mM Tris (pH 7.6)) just prior to use. ATP (0.2 mM) and β-mercaptoethanol (0.5 mM) were added immediately following the centrifugation.

Preparation of Labeled Actins. Pyrene-labeled actin was prepared according to the method of Cooper *et al.* (1983). Fluorescein-labeled actin was prepared by the method of Takashi (1979). DED-labeled actin was prepared by the method of Takashi (1988). ϵATP-labeled actin was prepared by the method of Root and Reisler (1992). The extent of labeling for each actin−dye complex was determined by using the molar extinction coefficients $\epsilon_{344} = 2.2 \times 10^4\ M^{-1}\ cm^{-1}$ for pyrenyl−actin, $\epsilon_{492} = 6.0 \times 10^4\ M^{-1}\ cm^{-1}$ for fluorescein−actin, and $\epsilon_{334} = 4.8 \times 10^3\ M^{-1}\ cm^{-1}$ for DED−actin. The concentration of each fluorescently labeled actin was determined by a Bradford assay (1976). The labeling stoichiometry of actin with the probes varied between 0.7 and 0.9 probe/actin for pyrene, 0.4 and 0.7 for fluorescein, and was 1.0 for DED attached to actin. The extent of ϵATP incorporation into actin was not measured.

Fluorescence Measurements. Fluorescence intensities were measured in a Spex fluorolog spectrophotometer (Spex Industries, Inc., Edison, NJ). Actin polymerization was monitored by the enhancement of pyrenyl−actin fluorescence (Kouyama & Mihashi, 1981). Polymerization of pyrene-labeled Ca- or Mg-G-actin (3.0 μM) in the presence of IgG (between 0 and 9.0 μM) was induced by the addition of one of the following reagents: $MgCl_2$ (3.0 mM), $CaCl_2$ (6.0 mM), NaCl (100 mM), or S-1 (4.5 μM). IgG-induced changes in actin conformation were observed by monitoring the changes in the emission spectra (fluorescence intensities and λ_{max}) of fluorescent probes located at different sites on actin. The concentration of labeled actins in these measurements was 3.0 μM, and that of IgG, when present, was 9.0 μM in solutions containing ϵATP and 6.0 μM in all other cases. Excitation and emission wavelengths for pyrene−actin were 366 nm and 407 nm, and those for ϵATP−actin were 340 and 410 nm, respectively. DED actin was excited at 334 nm. λ_{max} for DED emission of the different forms of actin are given in Table 1.

Nucleotide Exchange. Actin-bound ϵATP was chased from the nucleotide site by the addition of 0.5 mM ATP to Ca-G-actin or 20 μM ATP to Mg-G-actin (3.0 μM) in their respective G-actin and Mg-G-actin buffers. The rate of exchange was monitored via quenching of ϵATP fluorescence

Table 1: IgG-Induced Changes in Actin Observed with Fluorescent Probes[a]

protein	probe	location	$\lambda_{max}/\lambda_{max,IgG}$ (nm)	F_{IgG}/F_0
Ca-G-actin	pyrene	Cys-374	no change	1.75
Ca-F-actin	pyrene	Cys-374	no change	1.50
Mg-F-actin	pyrene	Cys-374	no change	1.80
Ca-G-actin	ϵATP	nucleotide cleft	no change	1.20
Mg-F-actin	ϵATP	nucleotide cleft	no change	1.40
Ca-G-actin	DED	Gln-41	529/524	1.18
Mg-G-actin	DED	Gln-41	508/504	1.20
Ca-F-actin	DED	Gln-41	no change	1.16
Mg-F-actin	DED	Gln-41	505/510	1.19

[a] Fluorescence spectra of labeled actins (3.0 μM) were observed in the presence and absence of IgG in either G-actin buffer or Mg-actin buffer at 25 °C. Changes in the λ_{max} of probe emission due to the addition of IgG ($\lambda_{max,IgG}$) and the ratios of fluorescence intensities in the presence (F_{IgG}) and absence of IgG (F_0) are presented. The concentration of IgG added was 6.0 μM for all labeled actins and 9.0 μM for ϵATP. The emission wavelength for pyrene–actin was 407 nm, and that for ϵATP actin was 410 nm. The emission λ_{max} for DED-labeled Ca-F-actin was 524 nm. In different protein preparations, fluorescence values varied up to 20% for pyrene–actin titrations with IgG and between 5% and 10% for ϵATP– and DED–actins with IgG.

accompanying its release from G-actin into the surrounding medium. The decrease in ϵATP fluorescence with time was recorded at λ_{em} = 410 nm (λ_{ex} = 340 nm). Exchange rates were obtained by fitting these curves to a single-exponential expression.

Airfuge Binding Measurements. Binding of IgG (between 0 and 9.0 μM) to either Ca- or Mg-actin filaments (3.0 μM) was measured following the incubation of protein mixtures for 30 min at 25 °C. Ca- and Mg-G-actin were polymerized by either $CaCl_2$ (6.0 mM), $MgCl_2$ (3.0 mM), or NaCl (100 mM) for 30–60 min prior to IgG addition. Samples were then centrifuged for 20 min at 25 °C at 140000g in a Beckman airfuge. Following resuspension of pelleted proteins in the original solvent, the samples were denatured and run on 10% SDS–polyacrylamide gels (Laemmli, 1970). Densitometric scans of the Coomassie-stained gels were analyzed to determine the molar ratios of IgG bound to actin.

Immunological Assays. Titers of anti-(18–29) polyclonal antibodies were checked by enzyme-linked immunosorbent assays as described by Atherton and Hynes (1981) and DasGupta *et al.* (1990). Microtiter plates were coated with 5 μg of skeletal muscle G-actin per well. The alkaline phosphatase colorimetric assay was used to measure the amount of antibody bound to adsorbed actin. The optical density was monitored at 405 nm with a Molecular Devices (Menlo Park, CA) V_{max} microplate reader. Western blots of SDS–polyacrylamide gels were performed as described by Bulinski *et al.* (1983), except that the immunoreactive bands were visualized using the Amersham ECL (enhanced chemiluminescent) Western blotting detection reagent.

Analytical Ultracentrifugation. Analytical ultracentrifugation experiments were conducted at 25 °C in a Beckman Model E analytical ultracentrifuge equipped with a photoelectric scanning system. Data collected into IBM PC files were transferred to a VAX 11/780 computer for analysis. Ca- and Mg-G-actins were labeled with fluorescein (5-IAF) at Cys-374, and their sedimentation was monitored at 492 nm. This simplified the analysis of sedimentation boundaries since only actin and its complexes, but not free IgG, were detected at this wavelength. The runs consisted of pairs of either Ca-G-actin ± IgG or Mg-G-actin ± IgG sedimented at 56 000 rpm. Actin and IgG concentrations were 10 μM each. Ca-G-actin was sedimented in G-actin buffer (0.2 mM $CaCl_2$, 0.5 mM β-mercaptoethanol, 0.2 mM ATP, 5 mM Tris (pH 7.6)) and Mg-G-actin in Mg-G-actin buffer (50 μM $MgCl_2$, 100 μM EGTA, 0.5 mM β-mercaptoethanol, 0.2 mM ATP, and 5 mM Tris (pH 7.6)).

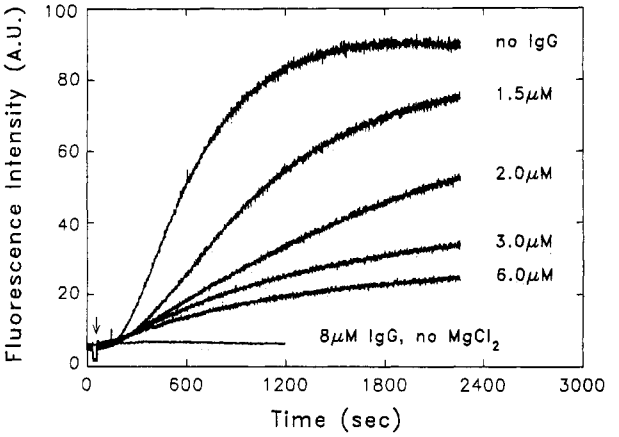

FIGURE 1: Effect of IgG on $MgCl_2$-induced actin polymerization. Pyrene-labeled Ca-G-actin (3.0 μM) was polymerized in G-actin buffer at 25 °C by the addition of 2.0 mM $MgCl_2$ in the absence and presence of IgG (between 1.5 and 6.0 μM). The increase in fluorescence of pyrene-labeled actin was monitored at 407 nm to indicate the extent of polymerization. The arrow indicates the time of $MgCl_2$ addition. IgG (8 μM) was also added to actin in the absence of $MgCl_2$ to check for antibody-induced actin polymerization. The fluorescence of all actin samples reached the same plateau level, when remeasured after 8 h.

Concentration Determinations. The following extinction coefficients were used to determine protein concentrations spectrophotometrically: actin (at 290 nm), $E^{1\%} = 11.5$ cm^{-1}; IgG (at 280 nm), $E^{1\%} = 15.0$ cm^{-1}.

RESULTS

IgG Binding to the Actin 18–29 Site Inhibits Polymerization. The addition of $MgCl_2$ to pyrene-labeled Ca-G-actin causes a rapid increase in fluorescence corresponding to the polymerization of actin induced by $MgCl_2$ (Kouyama & Mihashi, 1981). The effect of IgG on the $MgCl_2$-induced polymerization of pyrene-labeled G-actin is shown in Figure 1. It should first be noted that the addition of IgG alone to Ca-G-actin does not induce its polymerization. More importantly, the presence of antibody strongly inhibits the polymerization of Ca-G-actin induced by 2.0 (Figure 1), 3.0, and 4.0 mM $MgCl_2$ (not shown). Titration of Ca-G-actin with IgG results in decreasing rates of actin polymerization with increasing IgG concentrations. The final extent of polymerization in the presence of antibodies was checked 8 h later; in all cases, fluorescence plateaus similar to that observed for actin polymerized in the absence of IgG were reached (data not shown). Thus, the antibody decreases the rate but not the extent of actin polymerization by $MgCl_2$.

Because of the proximity of the 18–29 site to the nucleotide cleft and the high-affinity divalent cation site (Kabsch *et al.*, 1990), one possible explanation for the observed inhibition of actin polymerization is that the antibody binding inhibits the exchange of Ca^{2+} for Mg^{2+}, which precedes the polymerization (Gershman *et al.*, 1984). The divalent cation exchange step can be bypassed by either polymerizing Ca-G-actin with $CaCl_2$ or Mg-G-actin with

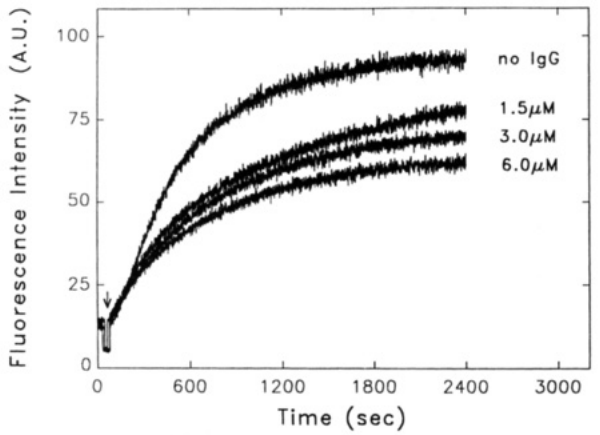

FIGURE 2: Effect of IgG on $CaCl_2$-induced actin polymerization. Pyrene-labeled Ca-G-actin (3.0 μM) was polymerized in G-actin buffer at 25 °C by the addition of 6 mM $CaCl_2$ in the absence and presence of IgG (between 1.5 and 6 μM). The increase in fluorescence of the pyrene-labeled actin was monitored at 407 nm to indicate the extent of polymerization. The arrow indicates the time of $CaCl_2$ addition. The fluorescence of all actin samples reached the same plateau levels, when measured after 8 h.

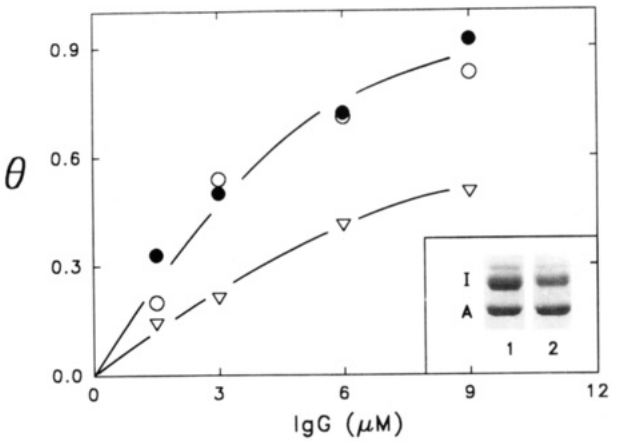

FIGURE 3: Binding of IgG to Mg- and Ca-F-actins. The binding was measured in airfuge pelleting experiments, as described in Materials and Methods. Densitometric scans of Coomassie-stained SDS−polyacrylamide gels were analyzed to determine the fraction of actin occupied by IgG (θ). IgG (between 1.5 and 9 μM) was pelleted with Mg-F-actin (3.0 μM) polymerized from either Ca-G-actin (●) or Mg-G-actin (○) by 3.0 mM $MgCl_2$ and with Ca-F-actin (3.0 μM) polymerized from Ca-G-actin (▽) with 6.0 mM $CaCl_2$. The inset shows a representative Coomassie-stained SDS−polyacrylamide gel (10%) of 6.0 μM IgG pelleted with 3.0 μM Mg-F-actin (lane 1) and 3.0 μM Ca-F-actin (lane 2).

$MgCl_2$. The impact of IgG on Ca-induced Ca-G-actin polymerization is shown in Figure 2. While IgG still inhibits this polymerization reaction at both 3.0 (not shown) and 6.0 mM $CaCl_2$, the effect is considerably weaker than that for $MgCl_2$-polymerized Ca-G-actin (Figure 1). However, when the polymerization of Mg-G-actin is induced by $MgCl_2$, the inhibition again is strong, similar to the effect shown in Figure 1 (data not shown). Clearly, the mechanism of antibody inhibition is not through the perturbation of divalent cation exchange at the high-affinity site. Polymerization of actin by other agents, either by monovalent salt (NaCl) or by myosin subfragment-1 (S-1), was not changed significantly by the presence of the antibody (data not shown).

Different Binding of Antibody to Mg- and Ca-Actins. The preceding observations could be explained by differences in antibody binding to the various forms of G-actin. Earlier ELISA experiments with antibodies to the 18−28 site on actin showed that they were approximately 25% less reactive with Ca-F-actin than with Mg-F-actin (Mejean *et al.*, 1988). Thus, cosedimentation studies were performed to assess the relative binding of the 18−29 antibody to Mg- and Ca-actin filaments in solution. As shown in Figure 3, the antibody binds approximately 40% better to Mg-F-actin than to Ca-F-actin. The binding of IgG to Mg-F-actin was the same whether Ca- or Mg-G-actin was used for obtaining the Mg polymer. This is not surprising since Mg^{2+} replaces Ca^{2+} at the high-affinity divalent metal binding site upon the addition of 3 mM $MgCl_2$ to Ca-G-actin (Gershman *et al.*, 1984). The binding results suggest that the differences seen in antibody inhibition of polymerization may reflect the stronger binding of antibody to Mg- than to Ca-G-actin, as seen in actin filaments. To test for such a possibility, information on the binding of IgG to Mg- and Ca-G-actin was needed.

Conclusive evidence for a difference in antibody binding to Mg- and Ca-G-actins was obtained from sedimentation velocity experiments. In order to simplify the observation of actin sedimentation in the presence of IgG and to avoid the need to distinguish between the boundaries of IgG and those of actin and the actin−IgG complexes at 280 nm, the actin was labeled with (5-IAF) fluorescein and monitored at

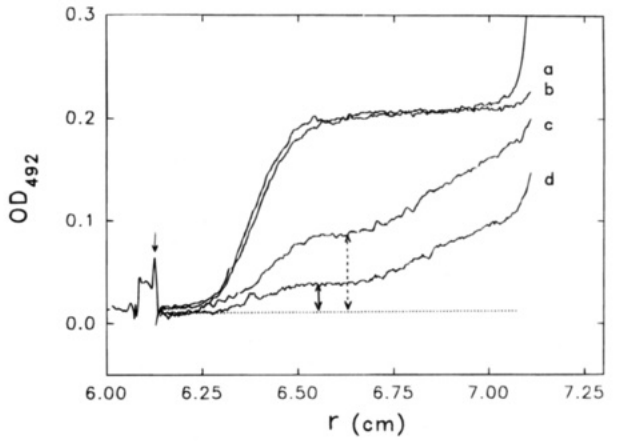

FIGURE 4: Binding of IgG to Ca- and Mg-G-actins. The sedimentation velocities of fluorescein-labeled Ca- and Mg-G-actins (10 μM) were measured in a Beckman Model E Analytical ultracentrifuge at 56 000 rpm and 20 °C. Curves a and b are representative sedimentation velocity boundaries of the Ca- and Mg-G-actins monitored at 492 nm. In the presence of IgG (10 μM), the G-actin population was partially depleted because of antibody binding and the faster sedimentation of G-actin−IgG complexes. Curves c and d show sedimentation boundaries for the mixtures of IgG with Ca- and Mg-G-actins, respectively. Arrows indicate monomeric actin plateaus; these plateaus are followed by the boundaries of the unpelleted heterogeneous actin−IgG complexes. An $s_{20,w}$ coefficient of approximately 4.0S was observed for monomeric actin populations, and the $s_{20,w}$ coefficients for IgG−actin complexes ranged between 7S and 9S, reflecting IgG−actin and IgG−$(actin)_2$ complexes. Scans were taken 58 (curves a and b) and 62 min (curves c and d) after reaching the final speed.

492 nm. In each experiment, the sedimentation of Ca- or Mg-G-actin in the presence of IgG was compared to that of G-actin alone. The results from these experiments are shown in Figure 4, which presents sedimentation boundaries taken at 58 (curves a and b) and 62 min (curves c and d) after reaching maximum centrifugation speed (56 000 rpm). A comparison of control curves (a and b) with Ca- and Mg-G-actin samples containing IgG (curves c and d) demonstrates that IgG binding to actin depletes, to a large extent,

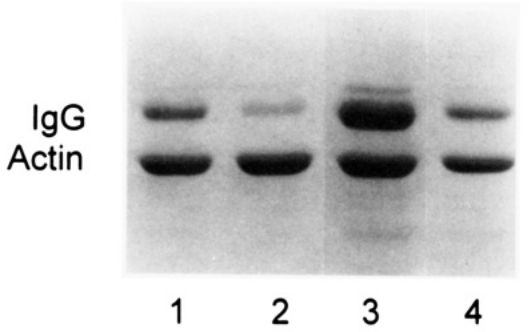

FIGURE 5: Effect of the strongly bound divalent cation on the binding of IgG to F-actin. The binding of IgG (6.0 μM) to F-actin (3.0 μM) obtained by polymerizing Mg-G-actin (lane 1) or Ca-G-actin (lane 2) with 100 mM NaCl was measured in pelleting assays as described in Materials and Methods. Lanes 3 and 4 show the binding of IgG to $MgCl_2$-polymerized Ca-G-actin in the absence and presence of 100 mM NaCl, respectively. The solvent was either G-actin buffer (5 mM Tris, 0.2 mM $CaCl_2$, 0.2 mM ATP, and 0.5 mM β-mercaptoethanol (pH 7.6)) or Mg-actin buffer (5 mM Tris, 0.2 mM ATP, 0.5 mM β-mercaptoethanol, 50 μM $MgCl_2$, and 100 μM EGTA (pH 7.6)).

the two solutions from monomeric actin sedimenting at a slower rate. A comparison of plateau regions in curves c and d reveals that there is significantly less Mg-actin monomer left in the partially sedimented Mg-G-actin−IgG sample (solid arrow, curve d) than there is Ca-actin monomer remaining in the Ca-G-actin−IgG mixture (dashed arrow, curve c). This demonstrates greater binding of IgG to Mg- than to Ca-G-actin.

The Metal Bound at the High-Affinity Divalent Cation Site Influences the Conformation of the 18−29 Loop. To test whether the changes in F-actin conformation sensed by the antibody are due to divalent cations at the high-affinity site, Ca- and Mg-G-actins were polymerized with NaCl (Figure 5) prior to IgG binding experiments. Under these conditions, the low-affinity cation sites are saturated by NaCl, while the high-affinity site contains either Ca^{2+} or Mg^{2+}. A comparison of lanes 1 and 2 in Figure 5 indicates that antibody binds better to the F-actin containing Mg^{2+} than that containing Ca^{2+} in the high-affinity site. This difference in antibody binding shows that the divalent cation in the nucleotide cleft affects the conformation of the 18−29 loop. In addition, the presence of NaCl dramatically reduces antibody binding to Mg-F-actin (Figure 5, lanes 3 and 4). A similar effect is seen with Ca-F-actin both in the absence and presence of 100 mM NaCl (compare Figure 3, lane 2, with Figure 5, lane 2), except that the overall binding of antibody to Ca-actin is lower than that to Mg-actin. The strong inhibition of IgG binding to actin in the presence of 100 mM NaCl provides a simple explanation for the lack of an IgG effect on G-actin polymerization by NaCl.

Antibody Binding to Actin Involves Charged Residues. In order to determine whether ionic strength or saturation of the low-affinity sites with monovalent cation affects antibody binding to actin, NaCl (between 0 and 100 mM) was added to Mg^{2+}-polymerized actin−IgG complexes just prior to their pelleting. As shown in Figure 6, the level of antibody binding to F-actin decreases with increasing NaCl concentration, reaching a minimum, <0.1 IgG−actin, at about 50 mM NaCl. This salt sensitivity of antibody−actin binding suggests that charged residues located in the antibody binding interface may be important for the interaction with the antibody. The likely candidates on actin were two acidic

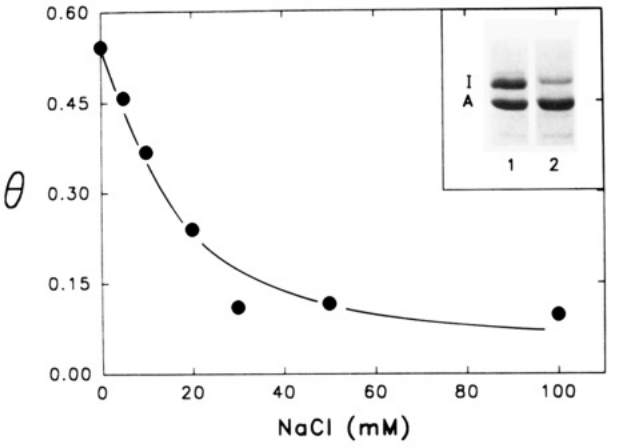

FIGURE 6: Effect of NaCl on IgG binding to F-actin. IgG (6.0 μM) was incubated with Mg-F-actin (3.0 μM) for 30 min at 25 °C. NaCl (between 0 and 100 mM) was added to actin just prior to centrifugation. The binding was measured in airfuge pelleting experiments, as described in Materials and Methods. Densitometric scans of Coomassie-stained SDS−polyacrylamide gels were analyzed to determine the fraction of actin occupied by IgG (θ). The inset shows representative lanes of a polyacrylamide gel used to determine the IgG binding to actin. IgG binding to F-actin is shown in the absence of NaCl (lane 1) and the presence of 50 mM NaCl (lane 2).

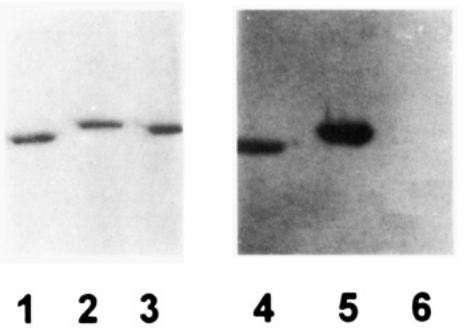

FIGURE 7: Comparison, by Western blot, of IgG binding to skeletal muscle α-actin, yeast wild-type actin, and the yeast actin mutant, D24A/D25A. Duplicate 10% SDS−polyacrylamide gels were either Coomassie-stained (lanes 1, 2, and 3) or electrotransferred to nitrocellulose and immunoblotted with (18−29) actin antiserum diluted 1:1000 in PBS (lanes 4, 5, and 6). Lanes 1 and 4 contain 5 μg of rabbit skeletal α-actin. Lanes 2 and 5 or 3 and 6 contain 5 μg each of yeast wild-type or the D24/A/D25A yeast mutant actin, respectively.

residues, Asp-24 and Asp-25, located in the hydrophilic loop contained within the actin 18−29 site (Kabsch *et al.*, 1990). In order to test this, the binding of antibody to skeletal muscle α-actin was compared to IgG binding to wild-type yeast actin and a yeast actin mutant in which the two aspartic acid residues were replaced with alanines (D24A/D25A). Western blots of the three actins were reacted with (18−29) antibody (Figure 7). The lack of antibody reactivity with the D24A/D25A mutant (lane 6) compared to the strong IgG reactivity with α-skeletal actin (lane 4) or wild-type yeast actin (lane 5) shows that the charged residues are critical for antibody binding.

Antibody Inhibits Nucleotide Exchange from the Cleft. The effect of divalent cations in the nucleotide cleft on the conformation of the 18−29 sequence on actin raised the possibility that antibodies bound to this site might in turn perturb the conformation of the nucleotide cleft. To address this question, the rate of ϵATP exchange from G-actin was monitored in ATP chase experiments. Since ϵATP fluores-

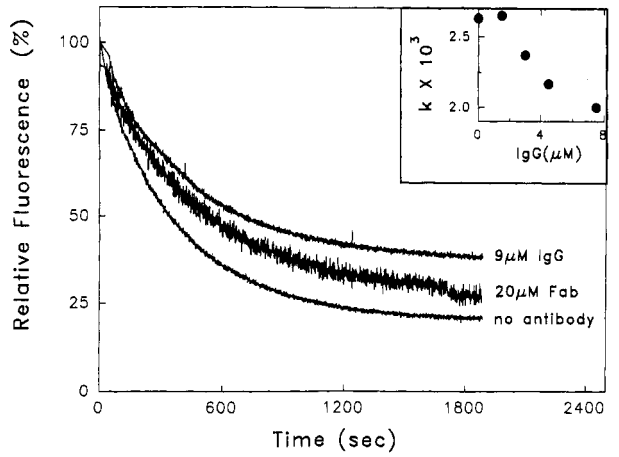

FIGURE 8: Time course of ϵATP exchange from Ca-G-actin in the presence of IgG and F_{ab}. ϵATP exchange from actin (3.0 μM) was observed by monitoring the decrease in ϵATP fluorescence as the analog was chased by ATP (0.5 mM) in G-actin buffer at 25 °C. Each data set was normalized to the fluorescence intensity of ϵATP−G-actin solution prior to the ATP chase. Excitation and emission wavelengths were 340 and 410 nm, respectively. The inset shows the observed rates ($k_{obs} \times 10^3$ s^{-1}) of nucleotide exchange in the presence of increasing concentrations of IgG. These rates were determined by fitting the data to a single-exponential expression.

cence is quenched when actin-bound ϵATP is released into solution, the rate of nucleotide exchange can be determined by measuring the rate of ϵATP quenching in the absence and presence of antibody. ATP chase experiments demonstrate that the presence of antibody (either IgG or its proteolytic fragment, F_{ab}) slows the rate of nucleotide exchange from Ca-G-actin (Figure 8). Nucleotide exchange rates were measured over a range of IgG concentrations (from 0 to 7.5 μM). Rate constants were determined by fitting these curves to a single-exponential equation. An approximately 30% decrease in the rate of nucleotide exchange was observed over this range of IgG concentrations (inset). A substantially larger decrease (about 2-fold) in the rates of nucleotide exchange was observed upon the binding of IgG (6.0 μM) to Mg-G-actin (not shown). However, despite the better binding of IgG to Mg-G-actin, and thus larger effects than in Ca-G-actin, these measurements are more difficult because of the rapid loss of the bound Mg-ϵATP from Mg-G-actin.

IgG-Induced Conformational Changes in Actin. The effect of antibodies on nucleotide exchange in G-actin prompted further testing of the conformational changes in actin induced by these antibodies. Three different fluorescent probes, namely, pyrene at Cys-374, ϵATP, and dansylethylenediamine (DED) attached to Gln-41, were used in order to monitor the impact of antibody on three corresponding sites on actin: The C-terminus, nucleotide cleft, and DNase I loop (subdomain-2) region. The results of these fluorescence measurements are listed in Table 1. In all cases, the fluorescence intensities are increased by antibody binding to actin. The increase in the pyrene fluorescence of G-actin is significant since the binding of IgG does not polymerize actin (Figure 1). Moreover, a similar fluorescence increase is observed in pyrenyl−F-actin. The IgG-induced increase in DED−G-actin fluorescence and the blue shift in its spectrum indicate that a portion of the DNase I loop implicated in actin monomer−monomer contacts (Strzelecka-Golaszewska *et al.*, 1993; Kabsch *et al.*, 1990; Holmes *et al.*, 1990) is shifted into a more hydrophobic environment when IgG binds to the 18−29 site on actin. Interestingly, IgG also perturbs this region in the polymerized actin (Mg-F-actin). An increase in actin-bound ϵATP fluorescence (Table 1) may suggest that the nucleotide is less exposed to solvent when IgG is bound. This would be consistent with the slower nucleotide exchange rate observed earlier (Figure 8). Notably, all of the IgG-induced conformational changes reported by the fluorescent probes occur in both G- and F-actin. At a qualitative level, this shows that the polymerization of actin does not block or greatly inhibit the propagation of conformational perturbation from the 18−29 sequence to the C-terminus, the nucleotide cleft, and the DNase I site on actin. Numerical analysis or titration of the observed effects has not been attempted in view of the differing degrees of actin saturation by IgG in the different forms of actin. Instead, the fluorescence results are taken as qualitative evidence for the conformational coupling between the 18−29 sequence and other sites on actin.

DISCUSSION

Previous studies have suggested an important role for the 18−29 site on actin in the weak actomyosin interactions in the presence of MgATP, both in the binding of actin to myosin and in the motile and myosin ATPase activating functions of actin (Adams & Reisler, 1993; Johara *et al.*, 1993; Miller & Reisler, 1994). Given the complexity of the actomyosin interface, with myosin binding via multiple contact sites on actin, it is difficult to dissect the effects of protein binding at any one site on actin. This is particularly true for the so-called nonspecific, weak electrostatic interaction sites for myosin (Rayment *et al.*, 1993), which encompass at least three seqences (1−7, 18−29, and 91−101) on actin (Johara *et al.*, 1993). Thus, for example, it is not obvious whether charge deletions in the 18−29 loop and the 1−7 segment affect other electrostatic interaction sites with myosin and/or the conformation of actin.

Despite its large size, the antibody to the 18−29 site provides a good probe for the possible structural coupling of this loop to other sites on actin and for conformational changes that may arise from the loop binding to proteins. The stronger inhibition of acto-S-1 ATPase activity than that of acto-S-1 binding by these antibodies is suggestive of such effects (Adams & Reisler, 1993). In order to assess the possiblity that changes in the 18−29 loop are transmitted to other regions on actin, several simple tests were conducted. These included the measurements of antibody effects on actin polymerization and nucleotide exchange on G-actin and on spectral probes placed at Cys-374, Gln-41, and in the nucleotide cleft. In this study, the 18−29 site is shown to actively participate in the dynamic response of actin to changes in the metal cation bound at the high-affinity divalent cation site. Antibody binding to actin inhibits its polymerization, slows the rate of nucleotide exchange, and also transmits conformational changes to other regions on actin.

The inhibition of $MgCl_2$-induced actin polymerization by the 18−29 IgG is particularly striking in view of the opposite effect of 1−7 IgG on this process (DasGupta *et al.*, 1990). The proximity of the 18−29 site to residues involved in stabilizing divalent cation and nucleotide binding in the cleft (Kabsch *et al.*, 1990) suggested that the antibody could inhibit the polymerization of actin by preventing the neces-

sary exchange of Ca^{2+} for Mg^{2+} at the high-affinity divalent cation site (Gershman *et al.*, 1984). However, the observation that the antibody strongly inhibited the polymerization of Mg-G-actin by $MgCl_2$, when no cation exchange was needed, demonstrated that the inhibition was not due to impaired divalent cation exchange. At this time, we cannot distinguish whether antibody binding to the 18−29 loop inhibits the polymerization of actin by sterically blocking the association of monomers or by inducing conformational changes at other sites on actin. The latter possibility is attractive since antibodies to a vicinal 1−7 epitope either have no effect on actin polymerization by $MgCl_2$ (F_{ab}) or accelerate it (IgG; DasGupta *et al.*, 1990).

The striking differences in the effect of antibody on Ca-G-actin polymerization compared to that observed for Mg-G-actin polymerization lead to the observation that the 18−29 loop is sensitive to the divalent cation bound in the nucleotide cleft. The observed difference in antibody binding to the 18−29 site in Ca- and Mg-actins reveals the flexibility of this loop and its conformational dependence on the high-affinity divalent cation in both G- and F-actins. Our sedimentation experiments, like previously reported ELISA studies (Mejean *et al.*,1988), clearly demonstrate that Mg-F-actin presents a more accessible 18−29 site to IgG than does the Ca-F-actin. We have now established that the conformation of this loop in G-actin is similarly impacted by the metal ion bound at the high-affinity site. Divalent cation-induced changes in local conformation previously have been reported in subdomain-2 (Strzelecka-Golaszewska *et al.*, 1993), at Val-201 in subdomain-4 (Mejean *et al.*, 1988), and at the actin C-terminus (Valentin-Ranc & Carlier, 1989; Carlier *et al.*, 1986; Estes *et al.*, 1987; Nowak *et al.*, 1988). Of particular interest is the electron microscopy study of Orlova and Egelman (1993), in which two states of actin filaments, flexible and rigid, were assigned to Mg- and Ca-F-actins, respectively. The flexibility change was associated with a rotation of subdomain-2 on actin. Our binding and spectroscopic results show that the changes in subdomain-2 and the 18−29 site are coordinated.

The lack of antibody inhibition of NaCl-induced actin polymerization clearly is due to the very low antibody binding to actin in the presence of 0.1 M monovalent salt. As indicated by experiments with the D24A/D25A yeast actin mutant, the strong ionic strength dependence of antibody binding can be traced to the contribution of Asp-24 and Asp-25 residues on actin to the interaction with IgG. The same acidic residues are also important for the weak, electrostatically dominated actomyosin interactions. Strong evidence for a direct role of these acidic residues in weak actomyosin binding comes from mutant actin studies in which replacement of these two acidic residues with either histidine (Johara *et al.*, 1993) or alanine residues (Miller & Reisler, 1994) strongly decreases actomyosin ATPase activity and the *in vitro* motility of actin filaments. In a previous antibody study, an additional catalytic role for the 18−29 actin site was suggested on the basis of the observation that blocking this site with antibody reduced the actin-activated S-1 ATPase activity of bound S-1 (Adams & Reisler, 1993).

The observations that actin-bound ϵATP fluorescence increases and the rate of nucleotide release from the cleft is slowed indicate that antibody binding to the 18−29 site impacts the nucleotide cleft. This is not surprising, considering the strong effect of the divalent cation in the cleft on antibody binding to the loop. It is also worth noting that S-1 (A2) binding to G-actin induces a similar decrease in the rate of nucleotide (ϵATP) release from the cleft (Kasprzak, 1993). The propagation of structural perturbation from the 18−29 loop is not restricted to the nucleotide cleft. Antibody-induced conformational changes reported by probes placed in subdomain-2 (Gln-41) and at the C-terminus (Cys-374) clearly show that communication to some of the same regions that sense changes in the nucleotide cleft can also be initiated from the 18−29 site. Of course, it is possible that these changes are mediated via the cleft. These findings are interesting because of some common features of S-1 and IgG interactions with the 18−29 site on actin, as discussed earlier. Moreover, none of the conformational effects of the 18−29 antibody could be detected with the 1−7 antibodies to actin (G. DasGupta and E. Reisler, unpublished results). Thus, the location of the epitope rather than the size of the antibody appears to be the main determinant of the structural changes observed here, although the latter possibility cannot be excluded.

There are indications that the plasticity of actin may play a role in actomyosin interaction. Myosin binding has been shown to increase the flexibility of actin filaments (Takebayashi *et al.*, 1977; Yanagida & Oosawa, 1978; Orlova & Egelman, 1993) in a manner similar to that seen when Ca^{2+} is absent from the actin filament or following P_i release. These observations suggest that myosin binding to actin filaments may also be disrupting subdomain-2−subdomain-3 contacts, which are important for stabilizing monomer associations along the long axis of actin filaments (Khaitlina *et al.*, 1993; Orlova & Egelman, 1993). It is easy but premature to speculate how such alterations in intermonomer contacts, originating from the myosin binding site, could contribute to cooperative effects in actin filaments. Additional characterization of the 18−29 site may lead to a better understanding of S-1-induced conformational changes in actin and their role in the contractile process.

ACKNOWLEDGMENT

We thank Drs. D. Drubin, D. Botstein, and K. Wertman for the mutant yeast actin strain and C. Miller for the gift of D24A/D25A mutant actin. We also thank Drs. P. Poon and M. Phillips for their assistance in analytical ultracentrifugation and Drs. M. Motoki and K. Seguro from Ajinomoto Co. Inc. (Kawasaki, Japan) for the gift of bacterial transglutaminase.

REFERENCES

Adams, S., & Reisler, E. (1993) *Biochemistry 32*, 5051−5056.
Aspenström, P., & Karlsson, R. (1991) *Eur. J. Biochem. 200*, 35−41.
Atherton, B. T., & Hynes, R. O. (1981) *Cell 25*, 133−141.
Bradford, M. M. (1976) *Anal. Biochem. 72*, 248−254.
Bulinski, J. C., Kumar, S., Titani, K., & Hauschka, S. (1983) *Proc. Natl. Acad. Sci. U.S.A. 80*, 1506−1510.
Carlier, M.-F., Pantaloni, D., & Korn, E. D. (1986) *J. Biol. Chem. 261*, 10778−10784.
Combeau, C., & Carlier, M. F. (1988) *J. Biol. Chem. 263*, 17429−17436.
Cook, R. I., Root, D., Miller, C., Reisler, E., & Rubenstein, P. A. (1993) *J. Biol. Chem. 268*, 2410−2415.
Cooper, J. A., Walker, S. B., & Pollard, T. D. (1983) *J. Muscle Res. Cell Motil. 4*, 253−262.

DasGupta, G., & Reisler, E. (1989) *J. Mol. Biol. 207*, 833−836.
DasGupta, G., & Reisler, E. (1992) *Biochemistry 31*, 1836−1841.
DasGupta, G., White, J., Phillips, M., Bulinski, J. C., & Reisler, E. (1990) *Biochemistry 29*, 3319−3324.
Estes, J. E., Selden, L. A., & Gershman, L. C. (1987) *J. Biol. Chem. 262*, 4952−4957.
Gershman, L. C., Newman, J., Selden, L. A., & Estes, J. E. (1984) *Biochemistry 23*, 2199−2203.
Godfrey, J. E., & Harrington, W. F. (1970) *Biochemistry 9*, 886−895.
Holmes, K. C., Popp, D., Gebhard, W., & Kabsch, W. (1990) *Nature 347*, 44−49.
Ishiwata, S., & Fujime, S. (1971) *J. Phys. Soc. Jpn. 30*, 302−303.
Johannes, F.-J., & Gallwitz, D. (1991) *EMBO J. 10*, 3951−3958.
Johara, M., Toyoshima, Y. Y., Ishijima, A., Koijima, H., Yanagida, T., & Sutoh, K. (1993) *Proc. Natl. Acad. Sci. U.S.A. 90*, 2127−2131.
Kabsch, W., Mannherz, H. G., Suck, D., Pai, E., & Holmes, K. C. (1990) *Nature 347*, 37−44.
Kasprzak, A. A. (1993) *J. Biol. Chem. 268*, 13261−13266.
Khaitlina, S. Y., Moraczewska, J., & Strzelecka-Golaszewska, H. (1993) *Eur. J. Biochem. 218*, 911−920.
Kinosian, H. J., Selden, L. A., Estes, J. E., & Gershman, L. C. (1991) *Biochim. Biophys. Acta 1077*, 151−158.
Kouyama, T., & Mihashi, K. (1981) *Eur. J. Biochem. 114*, 33−38.
Laemmli, U. K. (1970) *Nature 227*, 680−685.
Mejean, C., Boyer, M., Labbe, J.-P., Marlier, L., Benyamin, Y., & Roustan, C. (1987) *Biochem. J. 244*, 571−577.
Mejean, C., Hue, H. K., Pons, F., Roustan, C., & Benyamin, Y. (1988) *Biochem. Biophys. Res. Commun. 152*, 368−375.
Miller, C., & Reisler, E. (1994) *Biophys. J. 66*, A123.
Miller, L., Kalnoski, M., Yunossi, Z., Bulinski, J. C., & Reisler, E. (1987) *Biochemistry 26*, 6064−6070.
Miller, L., Phillips, M., & Reisler, E. (1988) *J. Biol. Chem. 263*, 1996−2002.
Milligan, R. A., Whittaker, M., & Sager, D. (1990) *Nature 348*, 217−221.
Muhlrad, A., Cheung, P., Phan, B. C., Miller, C., & Reisler, E. (1994) *J. Biol. Chem. 269*, 11852−11858.
Nowak, E., Strzelecka-Golaszewska, H., & Goody, R. (1988) *Biochemistry 27*, 1785−1792.
Orlova, A., & Egelman, E. H. (1992) *J. Mol. Biol. 227*, 1043−1053.
Orlova, A., & Egelman, E. H. (1993) *J. Mol. Biol. 232*, 334−341.
Rayment, I., Holden, H. M., Whittaker, M., Yohn, C. B., Lorenz, M., Holmes, K. C., & Milligan, R. A. (1993) *Science 261*, 58−65.
Reisler, E. (1993) *Curr. Opin. Cell Biol. 5*, 41−47.
Root, D. D., & Reisler, E. (1992) *Protein Sci. 1*, 1014−1022.
Spudich, J. A., & Watt, W. (1971) *J. Biol. Chem. 246*, 4866−4871.
Strzelecka-Golaszewska, H., Moraczewska, J., Khaitlina, S. Y., & Mossakowska, M. (1993) *Eur. J. Biochem. 211*, 731−742.
Sutoh, K., Ando, M., Sutoh, K., & Toyoshima, Y. Y. (1991) *Proc. Natl. Acad. Sci. U.S.A. 88*, 7711−7714.
Takashi, R. (1979) *Biochemistry 18*, 5164−5169.
Takashi, R. (1988) *Biochemistry 27*, 938−943.
Takebayashi, T., Morita, Y., & Oosawa, F. (1977) *Biochim. Biophys. Acta 492*, 357−363.
Valentin-Ranc, C., & Carlier, M.-F. (1989) *J. Biol. Chem. 264*, 20871−20880.
Vandekerckhove, J., & Weber, K. (1984) *J. Mol. Biol. 179*, 391−413.
Weeds, A., & Pope, A. B. (1977) *J. Mol. Biol. 111*, 129−157.
Yanagida, T., & Oosawa, F. (1978) *J. Mol. Biol. 126*, 507−524.